

P. Hoehner, "A statistical discrete-time model for the WSSUS multipath channel," *IEEE Transactions on Vehicular Technology*, vol. 41, pp. 461–468, Nov. 1992.

© 1992 IEEE. Personal use of this material is permitted. However, permission to reprint/republish this material for advertising or promotional purposes or for creating new collective works for resale or redistribution to servers or lists, or to reuse any copyrighted component of this work in other works must be obtained from the IEEE.

# A Statistical Discrete-Time Model for the WSSUS Multipath Channel

Peter Hoher, *Member, IEEE*

**Abstract**—The computation of the tap-gains of the discrete-time representation of a slowly time-varying multipath channel is investigated. Assuming the channel is wide-sense stationary with uncorrelated scattering (WSSUS), a known Monte Carlo-based method approximating the given scattering function (which fully determines the WSSUS channel) is extended by including filtering and sampling. The result is a closed-form solution for the tap-gains. This allows the efficient simulation of the continuous-time channel with, e.g., only one sample per symbol, and without explicit digital filtering. Finally, further advantages and remarks are indicated.

## I. INTRODUCTION

FUNDAMENTALLY, mobile radio communication channels are time-varying multipath channels. Since the performance of digital radio communication systems is strongly affected by multipath propagation in the form of scattering, reflection, and refraction, it is necessary to investigate their statistical behavior, which leads to "suitable" stochastic channel models.

The simplest nondegenerate class of processes which exhibits uncorrelated dispersiveness in time delay and Doppler shifts is known as the "wide-sense stationary uncorrelated scattering" (WSSUS) model introduced by Bello [1], [2], [3, ch. 7.1]. A linear superposition of uncorrelated echos is assumed, and wide-sense stationarity (at least short term). This simple analog channel model is fully determined by a two-dimensional scattering function in terms of the echo delay  $\tau$  due to multipath, and the Doppler frequency  $f_D$  due to the vehicle movement.

We will further assume that the number of uncorrelated paths is sufficiently large. Then, the quadrature components of the impulse response are Gaussian distributed according to the central limit theorem. A Gaussian WSSUS process (GWSSUS) is even stationary (GSUS). It was shown that the GWSSUS model fits to many channels of practical interest, such as the land mobile radio channel [4], [5] which is of particular interest in the following. It also applies to the troposcatter radio, HF radio, and indoor radio channels, as well as to many others.

Recently, Schulze presented a stochastic, Monte Carlo-based model to approximate the GWSSUS channel [6]. The principle is the generation of a single arbitrary realization of the GWSSUS process. Assuming ergodicity, each realization

Manuscript received March 26, 1991; revised August 2, 1991.

The author is with the Information Principles Research Lab, AT&T Bell Laboratories, Murray Hill, NJ 07974, on leave from the Institute for Communications Technology, German Aerospace Research Establishment, D-8031 Oberpfaffenhofen, Germany.

IEEE Log Number 9202462.

of the random process equivalently describes the channel. This analog model is appropriate for computer simulations; however, direct application requires sufficient oversampling to resolve the echos. Section II gives a brief review of the WSSUS channel model and Schulze's approximation thereof, and indicates implementation aspects in comparison to state of the art processing.

In the early 1970's, Forney proposed a discrete-time channel model [7], [3, ch. 6.3], that combines the effects of the transmitter filtering, the physical channel, the receiver filtering, and (symbol) sampling. This discrete-time model, a FIR filter with a tap-spacing according to the symbol period, is equivalent for the input/output representation. Forney showed that the optimum receiver filter is separable into a channel matched filter and a whitening filter, and he proved that the sampled output of the matched filter (and the output of any cascaded spectral-null-free filter) provides a set of sufficient statistics. Hence, this formulation is directly applicable for computer simulation without any further approximations.

In this paper we apply Forney's discrete-time representation to Schulze's Monte Carlo-based channel model, as introduced in [8]. In Section III, closed-form solutions for the time-varying FIR-filter tap-gains are derived and interpreted for the case of an optimum receiver filter, which is matched to the transmitter filter and the instantaneous channel impulse response, and for the case of a receiver filter matched to the transmitter filter only. Model inputs are the parameters of the scattering function and the impulse response of the transmitting filter.

We indicate that the FIR-filter is, in general, of infinite length even for finite-length echo delays, and that the tap-gains are correlated even under the supposition of uncorrelated scattering. These results are of theoretical interest and, furthermore, they may influence the filter and channel estimator design. An application is given for a land-mobile radio channel specified for the pan-European cellular GSM system [5].

A summary and concluding remarks appear in Section IV.

## II. THE CONTINUOUS-TIME CHANNEL MODEL

### A. WSSUS Channel Model

Throughout the paper we make use of the complex baseband notation. Let  $f(\tau; t)$  denote the impulse response of the channel, which is defined as the response at time  $t$  to a delta pulse which stimulated the channel at time  $t - \tau$ . The channel is assumed to be linear and slowly time-varying. Well-known "channel sounding" techniques for the direct

estimation of  $f(t; \tau)$  exists [2]. However, since the Doppler-spread is embedded in the complex envelope of the time-varying waveform, it is more suitable here to investigate the spectrum  $S(\tau; f_D)$  of  $f(\tau; t)$  defined as

$$S(\tau; f_D) = \int_{-\infty}^{+\infty} f(\tau; t) e^{-j2\pi f_D t} dt \quad (1)$$

where  $f_D$  is the Doppler frequency. The existence of (1) is assumed.

Theoretically, (1) and equivalent representations [1], [2] exactly describe the channel. However, from the practical point of view a stochastic description is necessary, since scattering, reflection, and inflection apparently causes a random, incoherent superposition of an infinite number of echos [6].

Another problem is the nonstationarity of the channel. For convenience, we adopt the useful separation into a "small-area" description and a "large-area" description to avoid a complicated channel model [2]. The small-area description, which is investigated in the following, represents the effects inside a limited area where wide-sense stationarity is assumed.

Because of the superposition, the quadrature components of the channel impulse response are Gaussian distributed according to the central limit theorem. Hence, it is sufficient to determine mean and correlation function. Without restriction, we assume in the following that the channel is zero mean ("Rayleigh fading"). A direct path ("Rice fading") has to be considered separately. The autocorrelation of  $S(\tau; f_D)$  is defined by

$$R_S(\tau, \tau'; f_D, f'_D) = \langle S(\tau; f_D) \cdot S^*(\tau'; f'_D) \rangle \quad (2)$$

where  $\langle \cdot \rangle$  is the ensemble average and the asterisk is the complex conjugate. Evaluation of (2) is difficult, but with the assumptions of wide-sense stationarity (according to the small-area description) and uncorrelated scattering, significant reduction is achieved:

$$R_S(\tau, \tau'; f_D, f'_D) = \delta(\tau - \tau') \delta(f_D - f'_D) \cdot P_S(\tau'; f'_D), \quad (3)$$

where  $\delta(t)$  is the delta function and  $P_S(\tau'; f'_D)$  is the delay-Doppler power spectrum, or scattering function for short. This WSSUS model, introduced by Bello [1], applies to many channels of practical interest [2], [4], [5].

### B. Monte Carlo Approximation of WSSUS Channel

In this subsection we briefly review Schulze's model to approximate the analog GWSSUS channel, and extend it to include frequency hopping.

Suppose the channel is composed of  $N$  echos. Each echo has an individual null-phase  $\theta_n$ , a delay  $\tau_n$ , and rotates with Doppler frequency  $f_{D_n}$ , where  $\theta_n$ , and  $\tau_n$ , and  $f_{D_n}$  are continuous random numbers, and  $1 \leq n \leq N$ . Hence, the instantaneous channel impulse response can be written as [6]

$$f(\tau; t) = \lim_{N \rightarrow \infty} \frac{1}{\sqrt{N}} \sum_{n=1}^N e^{j(\theta_n + 2\pi f_{D_n} t)} \cdot \delta(\tau - \tau_n) \quad (4)$$

in the limit for  $N \rightarrow \infty$ . The factor  $\sqrt{1/N}$  ensures convergence as  $N \rightarrow \infty$  according to the central limit theorem,

in which case the quadrature components are Gaussian distributed.

Equation (4) is a *phase modulation fading simulator* [9, fig. 1.7-1 (a)], and is based on the well-known principle of generating colored Gaussian noise by superposition of many sinusoids with uniformly distributed phases and random frequencies according to the desired noise spectrum. Equation (4) is two-dimensional, and is not restricted to deterministic arrivals  $\tau_n$  and/or deterministic Doppler frequencies  $f_{D_n}$ . Special cases of (4) include models by Iwasaki *et al.* [10] ( $f_D$  is stochastic,  $\tau = 0$ ), Lee [11, fig. 1-17, p. 43] ( $\tau$  is deterministic,  $f_D = 0$ ), and Jakes [9, sec. 1.7.1] ( $f_D$  is deterministic,  $\tau = 0$ ).

The amplitude weights of the complex sinusoids are not a function of the delay power spectrum or the Doppler spectrum [1], [12], [3], but are all equal. Their values,  $1/\sqrt{N}$ , are chosen so that the total average power is one, independent of the number of echos,  $N$ . The reason why we do not want the amplitudes to become involved is that the WSSUS model is statistically completely determined by the scattering function, and not primarily by the amplitudes and delays of the different paths. In this sense (4) differs from *quadrature amplitude modulation fading simulators* [9, fig. 1.7-1 (b)] investigated by Bello [1] and Turin *et al.* [12], among others [3], [4]. Also, the latter models are limited to produce rational forms of the fading spectrum [9], whereas the spectra encountered in mobile radio are generally nonrational [9].

In Appendix I, we show that the scattering function,  $P_S(\tau; f_D)$ , is proportional to the probability density function (pdf)  $p(\tau, f_D)$ . Hence, a simulation run is initialized by realizing  $\tau_n$  and  $f_{D_n}$  according to  $p(\tau, f_D)$ , and  $\theta_n$  according to a uniform distribution in  $[0, 2\pi)$ , where  $1 \leq n \leq N$ . Then, (4) approximates the GWSSUS model, and is exact provided that  $N$  approaches infinity.

Note that the realization of the random process has to be computed before the simulation starts. It contains, on the average, the same statistics as any other realization of possible outcomes because of ergodicity. In practice, however, for small  $N$ , it is advisable to compute new random samples from time to time, because this improves the statistic. Computing a new realization is equal to perfect frequency hopping (FH). It is straightforward to extend (4) to the case of real FH (i.e., hopping in a finite bandwidth), which is of practical interest in modem design. Since a carrier frequency shift,  $f_{\text{hop}}(t)$ , corresponds to a rotation in the time domain,  $f(\tau; t) \cdot \exp(j2\pi f_{\text{hop}}(t)\tau)$ , we obtain

$$f(\tau; t) = \lim_{N \rightarrow \infty} \frac{1}{\sqrt{N}} \sum_{n=1}^N e^{j(\theta_n + 2\pi f_{D_n} t + 2\pi f_{\text{hop}}(t)\tau_n)} \cdot \delta(\tau - \tau_n). \quad (5)$$

Note that (5) is of marginable extra complexity compared to (4).

The technique of realizing (4) and (5) by generating nominally uniformly distributed, pseudo-random variates and the weighting of such variates to establish the required distribution function is the basis of Monte Carlo simulation [13], [14].

Implementation aspects and a comparison with other channel models are discussed in the next subsection.

### C. Implementation Aspects and Comparison with Common Channel Model

As indicated, the phases  $\theta_n$ , the Doppler frequencies  $f_{D_n}$ , and the delays  $\tau_n$ , where  $1 \leq n \leq N$ , have to be established with distributions  $p(\theta)$  and  $p(\tau, f_D)$ , respectively, before the simulation starts. As usual, we assume  $\tau$  and  $f_D$  to be mutually independent [2], [5], hence  $p(\tau, f_D)$  reduces to the product of two first-order (marginal) pdf's  $p(\tau)$  and  $p(f_D)$ , where  $p(\tau)$  is proportional to the delay power spectrum, and  $p(f_D)$  is proportional to the Doppler power spectrum, as derived in Appendix I. According to the Monte Carlo principle, it is convenient to establish a (portable) uniformly distributed noise generator with outputs  $u_n \in [0, 1)$ , and to calculate  $v_n$  by a functional transformation

$$v_n = g_v(u_n) = P_v^{-1}(u_n); \quad 0 \leq u_n < 1 \quad (6)$$

where  $v_n$  is a substitute for  $\theta_n$ ,  $f_{D_n}$ , and  $\tau_n$ , respectively, and the memoryless nonlinearity  $g_v(u_n)$  is the inverse of the desired cumulative distribution function (cdf) [14].

As a first example, consider the one-sided exponentially distributed pseudo-random variate  $v_n = \tau_n$ , a model which is often used for the delay power spectrum [4], [5]:

$$p_\tau(\tau) = a \cdot e^{-\tau/b}, \quad \text{for } 0 \leq \tau \leq c. \quad (7)$$

Direct application of (6) leads to

$$\begin{aligned} g_\tau(u_n) &= -b \cdot \log_e(1 - u_n(1 - e^{-c/b})) \\ &\approx -b \cdot \log_e(1 - u_n), \quad \text{for } c \gg b. \end{aligned} \quad (8)$$

Another example is the so called "Jakes spectrum", which models the Doppler power spectrum in isotropic scattering ( $v_n = f_{D_n}$ ) [9], [4], [5]:

$$p_{f_D}(f_D) = \frac{1}{\pi f_{D_{\max}} \sqrt{1 - (f_D/f_{D_{\max}})^2}} \quad (10)$$

$$g_{f_D}(u_n) = f_{D_{\max}} \cdot \cos(2\pi u_n); \quad |f_D| < f_{D_{\max}} = v/\lambda \quad (11)$$

where  $f_{D_{\max}}$  is the maximum Doppler frequency, which depends on the vehicular velocity  $v$  and the wavelength  $\lambda$ . We refer to these examples in Section III-C. Now let us relate (4) and (5) to the quadrature amplitude modulation fading model, which is commonly used, and can be written as [1], [12], [3]

$$f(\tau; t) = \sum_{n=1}^N \beta_n(t) e^{j\theta_n(t)} \delta(t - \tau_n(t)) \quad (12)$$

where  $\beta_n(t)$ ,  $\theta_n(t)$ , and  $\tau_n(t)$  are the  $N$  path amplitudes, phases, and delays, respectively. From the implementation aspect, two solutions of (12) are conceivable: the first solution is an alternative Monte Carlo approach, however, this requires that both a first-order distribution (here:  $p(\tau)$ ) and a (Doppler) power spectrum have to be specified, which is much more involved [14]; the second solution is to filter each tap  $c_n(t)$  independently according to the desired Doppler power

spectrum. This requires  $N$  independent filters. We refer to this as the "filter approach" afterwards. We claim that the Monte Carlo model includes the following advantages compared to the filter approach.

1) The computation is faster, because it is not necessary to explicitly implement a digital filter. Also, only uniformly distributed inputs  $u_n$  are required during the simulation setup, instead of Gaussian variates during the simulation run (despite this, in both cases further reduction is possible by generating channel samples according to the sampling theorem, and to interpolate them).

2) The filter design is easier, and reduces to the computation of transformation (6). This design rule is much easier than common (IIR or FIR) filter design rules, which typically involve cascading, decimation and interpolation, or a frequency transformation. Concerning the Doppler spread, the filter design is in the frequency domain. Numerical instabilities principally do not occur even for a very low cutoff-frequency/symbol-rate ratio.

3) The filter design is believed to be exacter for comparable numerical effort. The  $(\tau, f_D)$ -variates are weighted according to the distribution  $p(\tau, f_D)$ . A relatively low number of realizations,  $N$ , is sufficient to guarantee that the moments of the realization are close to the moments of the desired distribution. Also, the cutoff frequency,  $f_{D_{\max}}$ , is exact.

4) The Monte Carlo model is easier to handle and more flexible. This is especially obvious in the case of (real or perfect) FH, which can be achieved at marginal overhead. Real FH is difficult to achieve in the filter approach, because changing the system state and acquiring acquisition are difficult if one does not want running multiple correlated channels in parallel.

To manifest these statements, we show some numbers to give an idea of the complexity: eighth-order IIR filters [15] or sixty fourth order FIR filters are reported in the literature to model a flat fading channel, whereas only about  $N = 10$  echos are necessary<sup>1</sup> to generate the Rayleigh fading process with the proposed Monte Carlo approach. Both models, an eighth-order IIR filter realized with four cascaded second-order subfilters in third-canonical form [15] and the Monte Carlo model of interest [6], were programmed as COMPLEX FUNCTION's in Fortran. On a SUN SPARK station 2, the average CPU time for  $10^6$  subroutine calls (i.e., the generation of  $10^6$  realizations of a complex Rayleigh fading process, without any interpolation to speed up) was found to be 182.2 s for the first model, and about half of the time (89.4 s) for the latter model with  $N = 10$  echos. (The effort is almost linear in  $N$ . The numbers include initialization, and are obtained for an optimized compiler. No sine/cosine tables were used. Double precision was found to be necessary for the first model. No FH included.) Hence, despite advantages 2–4 noted above, computation is faster for Rayleigh fading. If the channel is frequency-selective and/or with real FH, the advantages are even more obvious.

For all the variants discussed so far, whether based on (4) or (12), an (exact) equivalent discrete-time channel representation can be computed, which allows simulations with down to one sample per symbol, without quantization of the echo delays.

<sup>1</sup>From the work of Bennet and Slack it follows that the Rayleigh approximation is quite good for  $N \geq 6$  [9, pp. 68–69].

### III. THE DISCRETE-TIME CHANNEL MODEL

In this section we derive and compare the equivalent discrete-time channel models for the cases of an optimum receiver filter and a suboptimum receiver filter, respectively, on the basis of the Monte Carlo approximation.

We assume a linear modulation scheme. In Fig. 1,  $\{I_k\}$  is the complex data sequence,  $g(t)$  is the time-invariant impulse response of the transmitter filter,  $s(t)$  and  $r(t)$  is the transmitted and received signal, respectively,  $n(t)$  an additive white Gaussian noise process, and  $T$  is the symbol duration. The time-variant overall transmitter plus channel impulse response is

$$h(\tau; t) = g(t) * f(\tau; t) = \int_{-\infty}^{+\infty} g(\tau - \tau') \cdot f(\tau'; t) d\tau'. \quad (13)$$

#### A. Optimum Adaptive Receiver Filter

The optimum receiver filter is known to be a matched filter (MF) adapted to  $h(\tau; t)$  [7], [3], provided the maximum Doppler frequency is much smaller than the data rate (slow channel assumption). The MF output,

$$y_k = y(t|_{kT}) = y(t = kT) = \sum_j I_j \cdot x_k^{(k-j)} + n'_k \quad (14)$$

provides a set of sufficient statistics after symbol-rate sampling, compare Fig. 1(a). The sampled impulse response of the overall channel including transmitter filter, the physical channel, and the receiver filter

$$x_k^{(l)} = x_k^{(k-j)} = \int_{-\infty}^{+\infty} h^*(\tau - jT; t|_{kT}) \cdot h(\tau - kT; t|_{kT}) d\tau = x_k^{(j-k)*} \quad (15)$$

is the sampled time-variant autocorrelation of  $h(\tau; t|_{kT})$ , where  $k$  is the time index and  $l = k - j$  the time dispersion.  $n'_k$  in (14) is the colored noise process of the MF output. Because of symmetry, the  $z$ -transform of  $x_k^{(l)}$

$$X_k(z) = \sum_{l=-L}^L x_k^{(l)} z^{-l} = F_k(z) \cdot F_k^*(z^{-1}) \quad (16)$$

factors into  $F_k(z)$  and  $F_k^*(z^{-1})$ , where  $F_k(z)$  is a polynomial of degree  $L$ , with  $L$  being a positive integer such that  $x_k^{(l)}$  is zero for  $|l| > L$ . The corresponding time function is  $f_k^{(l)}$  with  $0 \leq l < L$ , and is related to  $x_k^{(l)}$  according to [3]

$$x_k^{(l)} = \sum_{j=0}^{L-l} f_k^{(j)*} \cdot f_k^{(j+l)}; \quad |l| \leq L. \quad (17)$$

A filter with  $z$ -transform  $1/F_k^*(z^{-1})$  after the MF decorrelates the noise sequence  $n'_k$ , and is thus called a whitening filter (WF). Usually, the minimum phase condition is selected out of the  $2^L$  possibilities [7], [3]. The overall impulse response is  $f_k^{(l)}$ ,  $0 \leq l \leq L$ , and the WF output signal is

$$z_k = \sum_{l=0}^L f_k^{(l)} \cdot I_{k-l} + \eta_k \quad (18)$$

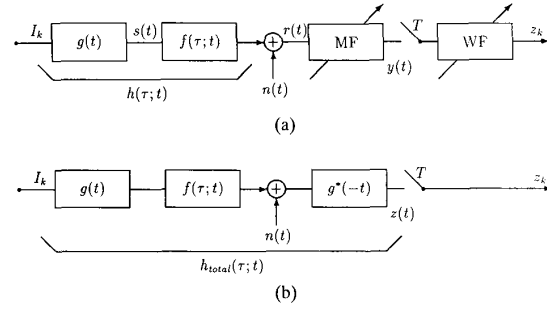


Fig. 1. Overall baseband model for communication over WSSUS fading multipath channels with transmitter filtering, WSSUS channel, additive noise, receiver filtering with (a) optimum or (b) nonadaptive filter and sampling.

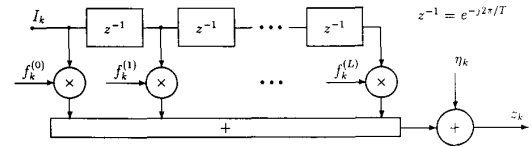


Fig. 2. Equivalent discrete-time channel model which represents the overall transmission model.

where  $\{\eta_k\}$  is, by definition, a white noise process. (14) and (18) are known as the *equivalent discrete-time channel models with colored or white noise* [7], [3], respectively, see Fig. 2. The  $f_k^{(l)}$  are the  $L + 1$  complex tap-gains of this FIR-filter representation, where  $0 \leq l \leq L$ . Note that the tap-spacing is exactly the sampling period ( $z^{-1} = e^{-j2\pi/T}$ ).

Now, we are able to apply the discrete-time representation to Schulze's channel model. Applying Parseval's theorem to (15), we obtain

$$x_k^{(l)} = \frac{1}{2\pi} \int_{-\infty}^{+\infty} |H_k(\omega)|^2 e^{j\omega l T} d\omega; \quad |l| \leq L \quad (19)$$

where  $\omega = 2\pi f$ , and  $H_k(\omega)$  is the Fourier transform of  $h(\tau; kT)$  with

$$|H_k(\omega)|^2 = |G(\omega)|^2 \cdot |F_k(\omega)|^2. \quad (20)$$

$G(\omega)$  is the Fourier transform of the transmitter filter  $g(t)$ , and  $F_k(\omega)$  is the instantaneous channel transfer function of  $f(\tau; t)$  given by

$$F_k(\omega) = \lim_{N \rightarrow \infty} \frac{1}{\sqrt{N}} \sum_{n=1}^N e^{j\theta_n} e^{j2\pi f_{D_n} k T} e^{-j\omega \tau_n} \quad (21)$$

and hence

$$|F_k(\omega)|^2 = \lim_{N \rightarrow \infty} \frac{1}{N} \sum_{n=1}^N \sum_{m=1}^N e^{j(\theta_n - \theta_m)} e^{j2\pi(f_{D_n} - f_{D_m})kT} e^{-j\omega(\tau_n - \tau_m)}. \quad (22)$$

Substitution of (20) and (22) into (19) yields

$$x_k^{(l)} = \lim_{N \rightarrow \infty} \frac{1}{2\pi N} \sum_{n=1}^N \sum_{m=1}^N e^{j(\theta_n - \theta_m)} e^{j2\pi(f_{D_n} - f_{D_m})kT} \cdot \int_{-\infty}^{+\infty} |G(\omega)|^2 e^{j\omega \tau^{(l)}} d\omega \quad (23)$$

or in shorthand notation

$$x_k^{(l)} = \lim_{N \rightarrow \infty} \frac{1}{N} \sum_{n=1}^N \sum_{m=1}^N \Xi(\theta_n - \theta_m, f_{D_n} - f_{D_m}, k) \cdot \Psi(\tilde{\tau}(l), g(t)) \quad (24)$$

with

$$\tilde{\tau}(l) = \tau_m - \tau_n + lT \quad (25)$$

$$\Xi(\theta_n - \theta_m, f_{D_n} - f_{D_m}, k) = e^{j(\theta_n - \theta_m)} e^{j2\pi(f_{D_n} - f_{D_m})kT} \quad (26)$$

$$\Psi(\tilde{\tau}(l), g(t)) = \frac{1}{2\pi} \int_{-\infty}^{+\infty} |G(\omega)|^2 e^{j\omega\tilde{\tau}(l)} d\omega. \quad (27)$$

Equation (27) is a Fourier integral and can, therefore, be simplified as follows:  $|G(\omega)|^2 = G_{\text{total}}(\omega)$  corresponds to the time function

$$g(t) * g^*(-t) = g_{\text{total}}(t), \quad (28)$$

and hence

$$\Psi(\tilde{\tau}(l), g(t)) = g_{\text{total}}(t)|_{t=\tilde{\tau}(l)}. \quad (29)$$

Finally, we obtain

$$x_k^{(l)} = \lim_{N \rightarrow \infty} \frac{1}{N} \sum_{n=1}^N \sum_{m=1}^N \Xi(\theta, f_D, k) \cdot g_{\text{total}}(\tilde{\tau}(l)). \quad (30)$$

$g_{\text{total}}(t)$  is the impulse response of transmitter and receiver filtering.

It seems to be important to indicate the properties and conclusions from (30). The first term,  $\Xi(\theta, f_D, k)$ , determines the dynamics of the discrete-time model, whereas the second term,  $g_{\text{total}}(\tau_m - \tau_n + lT)$ , determines the spread in  $l$ . Note that for a given  $l$  only the difference  $\tau_m - \tau_n$  is of significance, and contributes to one or more tap-gains, depending on  $g(t)$ . Assume  $\tilde{\tau}(l) \neq iT \quad \forall m \neq n$ , where  $i$  is an arbitrary integer, i.e.,  $\tilde{\tau}(l)$  is not a multiple of the sampling period  $T$  for all pairs of echos  $(m, n)$ ,  $m \neq n$ . In this case the tap-gains are correlated, hence the *discrete-time model does not satisfy the uncorrelated scattering condition* even for uncorrelated echos. The reason is that the continuous-time random process  $\tau$  is represented by a discrete-time process with spacing  $T$ .

Another important result concerns the number of tap-gains,  $L + 1$ . If  $G(\omega)$  is *bandlimited*,  $g(t)$  is unlimited in time and, therefore,  $L$  is *infinite even for a finite maximum echo delay* [16]. In contrast, if  $g(t)$  is time-limited,  $L$  is finite if the maximum echo delay is finite too. Since the decay of the tails of  $x_k^{(l)}$  (and hence the "practical" length of  $L$ ) depends on the channel bandwidth, it may be advisable for realizations to use a "smooth" transmitting pulse with a small time/bandwidth product, such as a Gaussian pulse. We give examples in Appendix II.

### B. Mismatched (Fixed) Receiver Filter

The matched filter receiver is difficult to implement (the filter must be adaptive), to simulate (the number of operations in direct application is quadratic in  $N$ ), and to analyze (the relation between  $x_k^{(l)}$  and  $f_k^{(l)}$  is nonlinear). Furthermore, a perfect adaptation has been assumed so far.

It may also be advisable to investigate the case of a fixed receiving filter. One reason is that low-cost receivers sometimes make use of a nonadaptive receiving filter, e.g., which is matched to the fixed transmitting filter. This setup, which is optimal for slow flat fading, is investigated in the following, see Fig. 1(b). Similarities and differences to the matched filter approach are indicated.

Another reason is that the receiver filter often has to be simulated separately, e.g., to simulate a nonperfect adaptation. In this case, the receiving filter in Fig. 1(b) has to be replaced by an ideal low-pass filter. This setup has been investigated in [16], and can be applied to the following results with minor changes.

For a fixed receiving filter  $g^*(-\tau)$  and with (4) the overall impulse response can be written as

$$\begin{aligned} h_{\text{total}}(\tau; t) &= f(\tau; t) * g(\tau) * g^*(-\tau) \\ &= f(\tau; t) * g_{\text{total}}(\tau) \\ &= \lim_{N \rightarrow \infty} \frac{1}{\sqrt{N}} \sum_{n=1}^N e^{j(\theta_n + 2\pi f_{D_n} t)} \cdot g_{\text{total}}(\tau - \tau_n). \end{aligned} \quad (31)$$

Let  $L_-$  and  $L_+$  be positive integers such that  $h_{\text{total}}(\tau; t)$  is zero outside  $-(L_-)T \leq t \leq (L_+)T$ . Hence, assuming symbol rate sampling,<sup>2</sup>  $t = kT$ , we obtain in former notation

$$z_k = \sum_{l=-L_-}^{L_+} f_k^{(l)} I_{k-1} + n_k \quad (32)$$

with

$$\begin{aligned} f_k^{(l)} &= h_{\text{total}}(lT; kT) \\ &= \lim_{N \rightarrow \infty} \frac{1}{\sqrt{N}} \sum_{n=1}^N e^{j(\theta_n + 2\pi f_{D_n} kT)} \cdot g_{\text{total}}(lT - \tau_n). \end{aligned} \quad (33)$$

$n_k$  in (32) is a sample of the noise process  $n(t) * g^*(-t)$ . If  $n(t)$  is white, and if  $g_{\text{total}}(t)$  satisfies the first Nyquist-criterion, then  $n_k = \eta_k$  also is white. Equation (32) is referred to as the *equivalent discrete-time model for the case of a fixed receiver filter*. Compared to the matched filter receiver case the inner sum in (30) is simply dropped. Among the differences are that, in general, precursors occur in the case of a fixed receiver filter ( $L_- \neq 0$ ). Also, the response is not minimum phase, and cannot be optimized to be so. Furthermore, the relationship between  $f_k^{(l)}$  and  $f(\tau; t)$  now is linear. Hence,  $f_k^{(l)}$  is a complex, zero mean Gaussian process, i.e., the amplitude is Rayleigh distributed, and the phase is uniformly

<sup>2</sup>Extension to oversampling is straightforward. The output process does not necessarily provide a set of sufficient statistics. The  $z_k$ 's in Figs. 1(a) and 1(b) have not the same value.

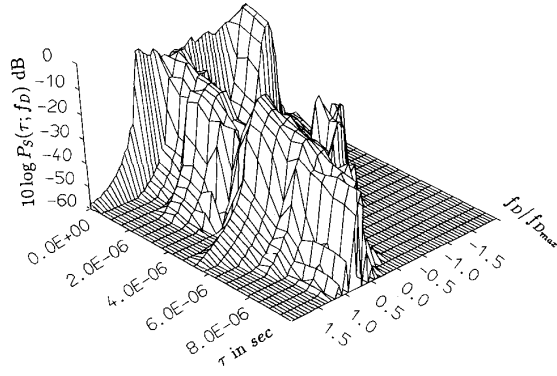


Fig. 3. Scattering function for a typical bad case in urban and suburban areas as specified for GSM.

distributed. The additive noise process is white only under special conditions.

### C. Example

As an example, Fig. 3 shows the scattering function of a land-mobile fading channel for a typical bad case in urban and suburban areas, as specified by CEPT-COST 207 for the pan-European cellular mobile system GSM [5]. Concerning the delay power spectrum, clusters with one-sided exponential delay are considered with a maximum delay of  $10 \mu\text{s}$ :

$$p(\tau) = \begin{cases} A \exp(-\tau/\mu\text{s}), & 0 \leq \tau < 5 \mu\text{s} \\ 0.5A \exp(5 - \tau/\mu\text{s}), & 5 \mu\text{s} \leq \tau < 10 \mu\text{s}. \end{cases} \quad (34)$$

The "Jakes spectrum" serves to model the Doppler power spectrum for the early isotropically arriving echos, whereas Gaussian shapes better reflect a preferred direction of the late echos [4], [5], as shown in (35) at the bottom of the page where  $G(A, f_1, f_2) = A \exp(-(f_D - f_1)^2 / (2f_2^2))$ ,  $B_1 = B - 10 \text{ dB}$ ,  $C_1 = C - 15 \text{ dB}$ .

The corresponding profiles of the equivalent discrete-time channel model with fixed receiving filter, (33), are presented in Fig. 4 for rectangular pulses, in Fig. 5 for raised-cosine pulses with rolloff  $r = 0.25$ , and in Fig. 6 for Gaussian pulses with  $\sigma_t = 0.3279T$ , which corresponds to an overall 99% bandwidth of  $1.25/T$ . In each case, symbol rate sampling with  $T = 3.7 \mu\text{s}$  is assumed [5].  $N = 500$  was chosen for illustration purposes. The advantage of using Gaussian pulses instead of raised-cosine pulses is obvious.

## IV. SUMMARY AND CONCLUSION

This paper applies the Monte Carlo-based analog channel model [6] to the discrete-time channel representation [7], [3].

We started with a short review of the WSSUS channel model, and its direct Monte Carlo approximation. Then, we

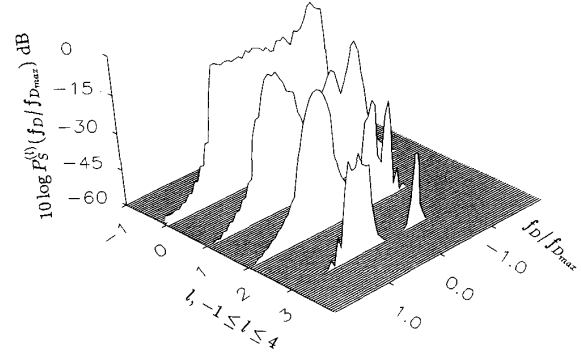


Fig. 4. Doppler power spectrum of  $f_k^{(l)}$ ,  $-1 \leq l \leq 4$ , for a typical bad case in urban and suburban areas (rectangular pulses,  $T = 3.7 \mu\text{s}$ ,  $N = 500$ ).

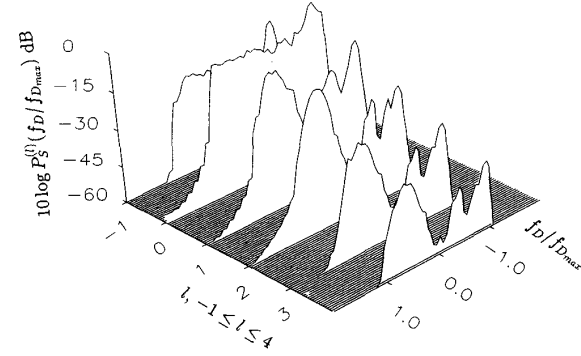


Fig. 5. Doppler power spectrum of  $f_k^{(l)}$ ,  $-1 \leq l \leq 4$ , for a typical bad case in urban and suburban areas (raised cosine pulses,  $r = 0.25$ ,  $T = 3.7 \mu\text{s}$ ,  $N = 500$ ).

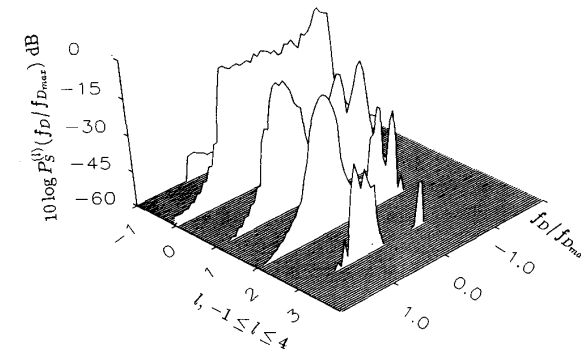


Fig. 6. Doppler power spectrum of  $f_k^{(l)}$ ,  $-1 \leq l \leq 4$ , for a typical bad case in urban and suburban areas (Gaussian pulses,  $\sigma_t = 0.3279T$ ,  $T = 3.7 \mu\text{s}$ ,  $N = 500$ ).

compared this model with other models and paid special attention to its advantages. Further, the equivalent discrete-

$$p(f_D) = \begin{cases} A/\sqrt{1 - (f_D/f_{D,\max})^2} & 0 \leq \tau < 0.5 \mu\text{s} \\ G(B, -0.8f_{D,\max}, 0.05f_{D,\max}) + G(B_1, 0.4f_{D,\max}, 0.1f_{D,\max}) & 0.5 \mu\text{s} \leq \tau < 2 \mu\text{s} \\ G(C, 0.7f_{D,\max}, 0.1f_{D,\max}) + G(C_1, -0.4f_{D,\max}, 0.15f_{D,\max}) & \tau \geq 2 \mu\text{s}, \end{cases} \quad (35)$$

time channel model of the input/output description including filtering and sampling was derived and compared for the cases of an optimum adaptive, and a fixed receiving filter. Examples were applied to a terrestrial cellular mobile radio channel.

We indicated that the "FIR"-representation of the discrete-time channel model is of infinite length when the transmitter filter is bandlimited. Hence, from the practical point of view pulses with a small time/bandwidth product are advantageous.

Also, we indicated the correlation between the complex tap-gains even for uncorrelated scattering on the physical channel. The knowledge of this correlation may improve a channel estimator. On the other side, it makes the analysis of the transmission system more involved.

We believe that the proposed model is faster than other approaches (no explicit digital filtering, no oversampling, uniform random variables during the simulation setup instead of Gaussian random variables during the simulation run), easier and exacter to design (simple transformation rule, exact cutoff frequency, no quantization of the echo delays  $\tau_n$ ), and finally easier to handle and more flexible (easy frequency hopping). Further reduction in complexity seems feasible by making use of more advanced Monte Carlo techniques such as importance sampling.

#### APPENDIX I

##### PROOF OF $p(\tau, f_D) \sim P_S(\tau; f_D)$

In the following we prove that the joint probability density function  $p(\tau, f_D)$  is proportional to the scattering function  $P_S(\tau; f_D)$  [8], [6], where  $\tau$  is the echo delay and  $f_D$  is the Doppler frequency.

We start with the autocorrelation of the system function  $F(f; t)$ , defined as

$$R_F(f, f'; t, t') = \langle F(f; t) \cdot F^*(f'; t') \rangle \quad (36)$$

compare (2). For the WSSUS process it follows that

$$R_F(\Omega; \Delta) = \langle F(f; t) \cdot F^*(f - \Omega; t - \Delta) \rangle \quad (37)$$

with  $\Omega = f - f'$  and  $\Delta = t - t'$ .  $F(f; t)$  can be approximated arbitrarily well by

$$F(f; t) = \frac{1}{\sqrt{N}} \sum_{k=1}^N e^{j\theta_k} e^{j2\pi f_{D_k} t} e^{-j2\pi f \tau_k} \quad (38)$$

if the number of echos,  $N$ , approaches infinity, see (4) and (21). After substitution in (37) and splitting it follows that

$$R_F(\Omega; \Delta) = \frac{1}{N} \left\langle \sum_{k=1}^N \sum_{l=1, l \neq k}^N \begin{aligned} & \cdot e^{j(\theta_k - \theta_l)} e^{j2\pi((f_{D_k} - f_{D_l})t + f_{D_l} \Delta)} \\ & \cdot e^{-j2\pi(f(\tau_k - \tau_l) + \Omega \tau_l)} \\ & + \sum_{k=1}^N e^{j2\pi f_{D_k} \Delta} \cdot e^{-j2\pi \Omega \tau_k} \end{aligned} \right\rangle. \quad (39)$$

If the terms are statistically independent and identically distributed with zero mean, the double sum is zero, and we

obtain

$$R_F(\Omega; \Delta) = \frac{1}{N} \left\langle \sum_{k=1}^N e^{j2\pi f_{D_k} \Delta} e^{-j2\pi \Omega \tau_k} \right\rangle. \quad (40)$$

Because of the linearity, ensemble average and summation are exchangeable, and because of the identical distribution it follows that

$$R_F(\Omega; \Delta) = \langle e^{j2\pi f_{D_k} \Delta} e^{-j2\pi \Omega \tau_k} \rangle, \quad (41)$$

and finally, with the definition of the first joint moment

$$R_F(\Omega; \Delta) = \int_{-\infty}^{+\infty} \int_{-\infty}^{+\infty} p(\tau', f'_D) e^{j2\pi f'_D \Delta} e^{-j2\pi \Omega \tau'} df'_D d\tau'. \quad (42)$$

Since  $R_F(\Omega; \Delta)$  and  $P_S(\tau'; f'_D)$  are related by [1]

$$R_F(\Omega; \Delta) = \int_{-\infty}^{+\infty} \int_{-\infty}^{+\infty} P_S(\tau'; f'_D) e^{j2\pi(f'_D \Delta - \Omega \tau')} df'_D d\tau', \quad (43)$$

a comparison with (42) leads to the desired result:

$$P_S(\tau; f_D) \sim p(\tau, f_D) \quad \text{Q.E.D} \quad (44)$$

By integration over  $f_D$  and  $\tau$ , we obtain that the mutual pdf's  $p(\tau)$  and  $(f_D)$  are proportional to the delay power spectrum  $P_S(\tau)$  and the Doppler power spectrum  $P_S(f_D)$ , respectively.

#### APPENDIX II

##### EXAMPLES FOR $x_k^{(l)}, |l| \leq L$

In this Appendix we give examples of the sampled autocorrelation  $x_k^{(l)}, |l| \leq L$ , for several transmitting filters  $g(t)$ .

##### A. For a time-limited pulse

$$g(t) = \frac{1}{T} \text{rect}(t/T), \quad g_{\text{total}}(t) = 1 - \frac{|t|}{T}, \quad \text{for } |t| \leq T \quad (45)$$

we obtain from (30):

$$x_k^{(l)} = \begin{cases} \lim_{N \rightarrow \infty} \frac{1}{N} \sum_{n=1}^N \sum_{m=1}^N \Xi(\theta, f_D, k) \cdot \left(1 - \frac{|\tilde{\tau}(l)|}{T}\right), & \text{for } |\tilde{\tau}(l)| \leq T \\ 0 & \text{else} \end{cases} \quad (46)$$

If the maximum echo delay is finite, e.g.

$$\Delta \tau_{\max} = \max_{n,m} |\tau_n - \tau_m| < \infty \quad (47)$$

then  $x_k^{(l)}$  is zero for  $|l| > L = \lceil \Delta \tau_{\max} / T \rceil$ , where  $\lceil \tau \rceil$  is the smallest integer greater or equal to  $\tau$ ,  $\tau \geq 0$ , since

$$|\tilde{\tau}(l)| = |\tau_m - \tau_n + lT| \leq T \quad (48)$$

from (46).

B. For a Bandlimited Nyquist-Pulse with Cosine Rolloff  $r$  [3]

$$g_{\text{total}}(t) = \frac{\sin \pi t/T}{\pi t/T} \frac{\cos r\pi t/T}{1 - (2rt/T)^2}, \quad (49)$$

we obtain from (30):

$$x_k^{(l)} = \lim_{N \rightarrow \infty} \frac{1}{N} \sum_{n=1}^N \sum_{m=1}^N \Xi(\theta, f_D, k) \cdot \frac{\sin \pi \tilde{\tau}(l)/T}{\pi \tilde{\tau}(l)/T} \frac{\cos r\pi \tilde{\tau}(l)/T}{1 - (2r\tilde{\tau}(l)/T)^2}. \quad (50)$$

$L$  is unbounded, at least theoretically, as long as  $\tilde{\tau}(l)$  is not a multiple of  $T$  for all pairs of echos. Note that the tails of  $x_k^{(l)}$  decay as  $1/\tilde{\tau}^3$ . The effective number of echos grows with decreasing rolloff  $r$ , that is, with more bandwidth efficiency.

C. For a Gaussian Pulse with Variance  $\sigma_t^2$

$$g_{\text{total}}(t) = \frac{1}{\sqrt{2\pi\sigma_t^2}} \exp\left(-\frac{t^2}{2\sigma_t^2}\right) \quad (51)$$

we obtain from (30):

$$x_k^{(l)} = \lim_{N \rightarrow \infty} \frac{1}{N} \sum_{n=1}^N \sum_{m=1}^N \Xi(\theta, f_D, k) \cdot \frac{1}{\sqrt{2\pi\sigma_t^2}} \exp\left(-\frac{(\tilde{\tau}(l)/T)^2}{2\sigma_t^2}\right). \quad (52)$$

The decay is exponential, which is much faster than with cosine rolloff Nyquist-pulses. This example shows that partial response pulses are of practical interest for data transmission over frequency-selective channels.

ACKNOWLEDGMENT

The author gratefully acknowledge discussions with H. Schulze concerning the Monte Carlo approximation.

REFERENCES

- [1] P. A. Bello, "Characterization of randomly time-invariant linear channels," *IEEE Trans. Commun. Syst.*, vol. CS-11, pp. 360-393, Dec. 1963.
- [2] J. D. Parsons and A. S. Bajwa, "Wideband characterisation of fading mobile radio channels," *Inst. Elec. Eng. Proc.*, vol. 129, pt. F, no. 2, pp. 95-101, Apr. 1982.

- [3] J. G. Proakis, *Digital Communications*. New York: McGraw-Hill, 2nd ed. 1989.
- [4] D. Bodson, G. F. McClure, and S. R. McConoughey, Eds., *Land-Mobile Communications Engineering*. New York: IEEE Press, 1984.
- [5] CEPT/COST 207 WG1, "Proposal on channel transfer functions to be used in GSM tests late 1986," COST 207 TD (86)51 Rev. 3, Sept. 1986.
- [6] H. Schulze, "Stochastic models and digital simulation of mobile channels" (in German), U.R.S.I./ITG Conf. in Kleinheubach 1988, Germany (FR), *Proc. Kleinheubacher Berichte* by the German PTT, Darmstadt, vol. 32, pp. 473-483, 1989.
- [7] G. D. Forney, "Maximum-likelihood sequence estimation of digital sequences in the presence of intersymbol interference," *IEEE Trans. Inform. Theory*, vol. IT-18, pp. 363-378, May 1972.
- [8] P. Hoeher, Coherent Reception of Trellis-Coded PSK-Signals on Frequency-Selective Mobile Radio Channels-Equalization, Decoding and Channel Estimation (in German). Duesseldorf, Germany: VDI Verlag, Fortschritt-Berichte, Series 10, no. 147, 1990.
- [9] W. C. Jakes, Ed., *Microwave Mobile Communications*. New York: Wiley, 1974.
- [10] K. Iwasaki, M. Shimada, T. Iida, and S. Shimoseko, "Computer simulation of digital modulation techniques for mobile/personal communications via satellite," *J. Radio Res. Lab.*, Japan, vol. 32, no. 135, pp. 1-14, Mar. 1985.
- [11] W. C. Y. Lee, *Mobile Communications Design Fundamentals*. New York: Macmillan, Inc., 1986.
- [12] G. L. Turin, F. D. Clapp, T. L. Johnston, S. B. Fine, and D. Lavry, "A statistical model for multipath propagation," *IEEE Trans. Veh. Technol.*, vol. VT-21, pp. 1-9, Feb. 1972.
- [13] J. M. Hammersley and D. C. Handscomb, *Monte Carlo Methods*. London: Methuen, 1964, reprinted 1975.
- [14] R. F. W. Coates, G. J. Jannacec, and K. V. Lever, "Monte Carlo simulation and random number generation," *IEEE J. Select. Areas Commun.*, vol. SAC-6, pp. 58-66, Jan. 1988.
- [15] H. Brehm, H. Stammmler, and W. Werner, "Design of a highly flexible digital simulator for narrowband fading channels," in *Signal Processing III: Theories and Applications*, I. T. Young, Ed., Amsterdam: Elsevier Science Publishers, North-Holland, EUSIPCO'86, pp. 1113-1116, 1986.
- [16] K. Pahlavan and J. W. Matthews, "Performance of adaptive matched filter receivers over fading multipath channels," *IEEE Trans. Commun.*, vol. 38, pp. 2106-2113, Dec. 1990.



**Peter Hoeher** (M'90) was born in Cologne, Germany, on April 5, 1962. He received the Dipl.-Ing. degree in electrical engineering from the Aachen University of Technology (RWTH), Aachen, Germany, in 1986, and the Ph.D. degree in electrical engineering from the University of Kaiserslautern, Germany, in 1990.

Since 1986 he has been a Research Assistant in the Institute for Communications Technology at the German Aerospace Research Establishment (DLR), Oberpfaffenhofen, Germany. His current interests are in power and bandwidth efficient transmission, particular in coding, equalization, and in synchronization for mobile radio. Dr. Hoeher received the 1990 Hugo-Denkmeier-Award.